

From magnetism to one-dimensional spin liquid in the anisotropic triangular lattice

Dariusz Heidarian,^{1,2} Sandro Sorella,^{1,2} and Federico Becca,^{1,2}

¹ *International School for Advanced Studies (SISSA), Via Beirut 2, I-34014 Trieste, Italy*

² *CNR-INFM-Democritos National Simulation Centre, Trieste, Italy.*

(Dated: September 14, 2021)

We investigate the anisotropic triangular lattice that interpolates from decoupled one-dimensional chains to the isotropic triangular lattice and has been suggested to be relevant for various quasi-two-dimensional materials, such as Cs_2CuCl_4 or $\kappa\text{-(ET)}_2\text{Cu}_2(\text{CN})_3$, an organic material that shows intriguing magnetic properties. We obtain an excellent accuracy by means of a novel representation for the resonating valence bond wave function with both singlet and triplet pairing. This approach allows us to establish that the magnetic order is rapidly destroyed away from the pure triangular lattice and incommensurate spin correlations are short range. A non-magnetic spin liquid naturally emerges in a wide range of the phase diagram, with strong one-dimensional character. The relevance of the triplet pairing for $\kappa\text{-(ET)}_2\text{Cu}_2(\text{CN})_3$ is also discussed.

PACS numbers: 75.10.-b, 71.10.Pm, 75.40.Mg

When cooling down the temperature, the majority of materials undergo phase transitions to ordered phases, that break some symmetry. Examples are ubiquitous in nature, e.g., magnets or superconductors, and define the paradigm in solid state physics. In the last years, a great effort has been done to determine and characterize new states of matter, which escape this conventional description. In this regard, one of the most intriguing case is given by the so-called spin liquids, namely insulating phases that cannot be adiabatically connected to any band insulators. [1] The concept of spin liquid was introduced by Fazekas and Anderson [2] and its possible connection with the low-doping regime of high-temperature superconductors was highlighted by Anderson. [3] The standard picture of a spin liquid is given by the resonating valence bond (RVB) ansatz, a superposition of configurations in which couples of spins form singlets but change partner from one configuration to the other. After a long period dominated by the (wrong) prejudice that spin liquids cannot be actually stabilized, today there is an increasing evidence that they can be obtained in both microscopic models and real materials. Spin-liquid behavior has been suggested in various compounds: in two-dimensional (2D) triangular lattices, [4, 5] in Kagome materials, [6] and more recently in three-dimensional hyper-Kagome antiferromagnets. [7]

The 2D triangular lattice is the simplest structure in which the nearest-neighbor super-exchange leads to frustration. However, it is well proved that ideal Heisenberg spins with antiferromagnetic interactions on such a lattice display an ordered spin configuration, even for the spin-half case. [8, 9] Nevertheless, due to strong quantum fluctuations, the magnetic order parameter is highly reduced from its classical value [9, 10] and small perturbations may destroy long-range order and drive the system towards a pure spin-liquid ground state. In this sense, a finite on-site repulsion U (or equivalently multi-spin interactions) may stabilize a magnetically disordered phase

close to the metal-insulator transition. [11, 12] Another very interesting possibility to further increase quantum fluctuations is to have different super-exchange couplings along different spatial directions. This latter case is particularly appealing because of its connection with various materials, such as Cs_2CuCl_4 and Cs_2CuBr_4 [13] or a family of quasi-2D organic compounds. [14]

In this Letter, we consider a spin-half Heisenberg model defined on the anisotropic triangular lattice:

$$\mathcal{H} = J \sum_{(i,j)} \mathbf{S}_i \cdot \mathbf{S}_j + J' \sum_{\{i,j\}} \mathbf{S}_i \cdot \mathbf{S}_j, \quad (1)$$

where $\mathbf{S}_i = (S_i^x, S_i^y, S_i^z)$ is the spin operator at the site i and (i, j) indicates nearest-neighbor sites along the $\mathbf{a}_1 = (1, 0)$ direction, while $\{i, j\}$ indicates nearest-neighbor sites along either $\mathbf{a}_2 = (1/2, \sqrt{3}/2)$ or $\mathbf{a}_3 = (-1/2, \sqrt{3}/2)$. Therefore, the model consists in one-dimensional (1D) chains coupled with zig-zag bonds J' . Here, we consider clusters with $N = L^2$ sites and periodic boundary conditions along $L\mathbf{a}_1$ and $L\mathbf{a}_2$. Recent works showed a strong *one-dimensionalization* [15] and gapless $S = 1/2$ excitations [16] in a wide regime of frustration $J'/J \lesssim 0.5$. The main limitation of these results is the inaccurate description of the magnetic correlations. In fact, works based upon series expansions [18, 19] showed that a magnetic spiral order may be present down to the 1D limit, with almost antiparallel spins along chains. The fact that the 1D disordered phase is unstable towards the formation of incommensurate magnetic order has been also suggested by perturbative approaches. [20, 21] The situation is far from being clarified and more work is needed to understand the nature of the ground state.

Before considering our variational Monte Carlo calculations, it is useful to present exact results by the Lanczos method on the 6×6 cluster, see Fig. 1. As already obtained in Ref. 22, we find a level crossing in the ground state; this is due to a change, around $J'/J \sim 0.825$, in the quantum number of the reflection symmetry. In addition

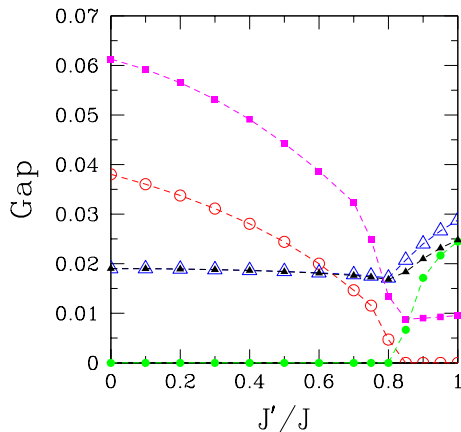


FIG. 1: (Color on-line) Exact energy gap for the 6×6 cluster as a function of the frustrating ratio J'/J . Full and empty circles indicate singlet states with $q = (0, 0)$ and different reflection symmetry (the data show a level crossing for $J'/J \sim 0.825$). Empty and full triangles indicate triplet excitations at $q = (\pi, \pi/3\sqrt{3})$ and $q = (\pi, \pi/\sqrt{3})$, respectively. Full squares indicate triplet excitations at $q = (3\pi/4, 0)$.

to ground-state properties, here we can also afford calculations for the important low-energy excited states. We find that the lowest triplet excitation has different quantum numbers for $J'/J \gtrsim 0.775$, where $q = (3\pi/4, 0)$, and for $J'/J \lesssim 0.775$, where $q = (\pi, \pi/\sqrt{3})$. Remarkably, in a wide regime, the low-energy spectrum shows a clear 1D character with two (almost) degenerate triplet excitations with $q_x = \pi$, namely $q = (\pi, \pi/\sqrt{3})$ and $q = (\pi, \pi/3\sqrt{3})$, see Fig. 1.

Let us now move to a detailed study of the Hamiltonian (1) by using a variational wave function (WF) approach that includes both magnetic correlations and electronic pairing. In the original RVB approach the variational WF can be obtained by applying the Gutzwiller projector \mathcal{P}_G that completely suppress doubly occupied sites to the ground state of a mean-field BCS Hamiltonian. [3] Within the same variational approach, a magnetic state is obtained by adding an external field in the BCS Hamiltonian and considering a suitable long-range spin Jastrow factor that introduces the correct spin-wave fluctuations, i.e., $\mathcal{J}_s = \exp\left(1/2 \sum_{i,j} v_{ij} S_i^z S_j^z\right)$. [23] The ground state of the mean-field Hamiltonian containing both electronic pairing and magnetism can be written in terms of a generalized complex pairing function $f_{i,j}^{\sigma_i, \sigma_j}$ that contains both singlet and triplet components, so that the full variational WF is given by: [23]

$$|\Psi\rangle = \mathcal{J}_s \mathcal{P}_G \exp \left\{ \frac{1}{2} \sum_{i,j, \sigma_i, \sigma_j} f_{i,j}^{\sigma_i, \sigma_j} c_{i, \sigma_i}^\dagger c_{j, \sigma_j}^\dagger \right\} |0\rangle, \quad (2)$$

where c_{i, σ_i}^\dagger creates an electron with spin σ_i on the site

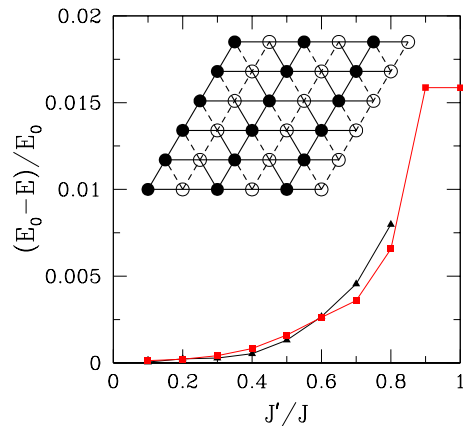


FIG. 2: (Color on-line) Accuracy for the energy on the 6×6 lattice, E_0 and E denote the exact and the variational energies. The WF with decoupled chains (black triangles) and the one with 2×1 structure and 120° order (red squares) are reported, see text for a detailed description. The example of the 2×1 structure for the sign of the nearest-neighbor sites is also reported: solid and dashed lines denote positive and negative pairing amplitudes, respectively.

i. At present, all variational approaches on the lattice have optimized the WF by considering few *short-range* parameters of the BCS Hamiltonian (e.g., the BCS pairing and/or hopping amplitudes), implying a *long-range* pairing function. Here, we generalize this variational approach without defining the mean-field BCS Hamiltonian. Instead, we directly optimize the pairing amplitude $f_{i,j}^{\sigma_i, \sigma_j}$. This approach allows us to have more variational freedom and, therefore, provides a much less biased ansatz to the ground state. Let us now discuss the symmetries that we use for this quantity. First of all, we consider independent (σ_i, σ_j) values for (\uparrow, \uparrow) , (\downarrow, \downarrow) , (\uparrow, \downarrow) , and (\downarrow, \uparrow) amplitudes. Then, in order to take into account magnetic correlations, we consider two different possibilities. The first one has a three-sublattice symmetry (suitable to the 120° order) and the second one has antiparallel spins along 1D chains and with two independent chains with different magnetic moment (suitable to describe the magnetic order for $J'/J \ll 1$). Despite these limitations, the correlated WF of Eq. (2), optimized in presence of the Jastrow factor \mathcal{J}_s , may show clear incommensurate spin-spin correlations, demonstrating that our approach is highly flexible and allows us to describe non-trivial spin correlations. In summary, for each bond and each spin case, we have three (two) independent complex numbers for the first (second) case. Finally, a 2×1 structure that implies an extra sign factor (+1 or -1) for each $f_{i,j}^{\sigma_i, \sigma_j}$ is considered [17] for the case of three sublattices, see Fig. 2 for the sign convention of nearest-neighbor sites. Periodic or antiperiodic boundary conditions on $f_{i,j}^{\sigma_i, \sigma_j}$ are chosen, depending on L . Although

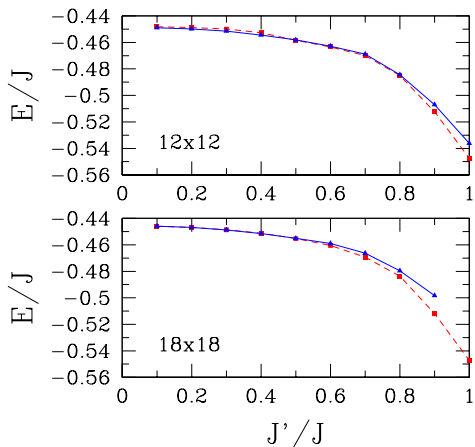


FIG. 3: (Color on-line) Energy per site for the 12×12 (upper panel) and the 18×18 (bottom panel) for the WF with three-sublattice magnetization and 2×1 structure (red squares) and with two decoupled chains (blue triangles). See text for a detailed description of the WFs.

the WF breaks the spin $SU(2)$ symmetry, the actual value of the total spin square $\langle S^2 \rangle$ is as small as 0.07 for the 18×18 cluster. The fundamental ingredients are the presence of the 2×1 structure for the signs of the pairing, relevant for $J' \sim J$, and the direct optimization of $f_{i,j}^{\sigma_i, \sigma_j}$ (containing both singlet and triplet components), which is afforded here for the first time. In the isotropic case, we obtain excellent results, which give an energy per site $E/J = -0.5470(1)$ in the thermodynamic limit, very close to our estimation of the exact value $E/J = -0.551(1)$ (which is extracted with the variance extrapolation of WFs with zero and one Lanczos step [24]) and much lower than previous estimates $E/J \sim -0.53$. [25, 26]

In Fig. 2, we report the accuracy of the two WFs (with three-sublattice or two-chain structure) for the 6×6 lattice. The full optimization of the pairing function allows us to reach a very good accuracy in the whole range of our interest and, in particular, for $J'/J \lesssim 0.5$. We notice that the level crossing present in exact calculations (see Fig. 1) is also present in the energy of the two variational WFs, although it is shifted to $J'/J \sim 0.6$. In the case of a first-order transition, there is a macroscopic energy difference between the stable and the unstable states in both regions across the transition point. However, by increasing the system size, we observe that the two energies merge for small frustrating ratios, namely $J'/J \lesssim 0.6$, see Fig. 3. This indicates that the transition becomes continuous in the thermodynamic limit. The tiny energy difference between the two WFs for $J'/J \lesssim 0.6$ suggests an effective chain decoupling. Indeed, the two variational WFs are compatible with a continuous transition: at the critical point, the two states coincide and have vanishing

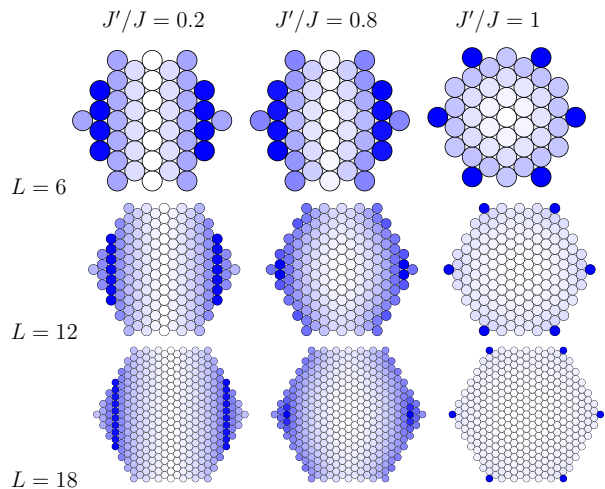


FIG. 4: (Color non-line) Static spin-spin correlations $S(q)$ for different lattice sizes $N = L \times L$ and frustrating ratios J'/J . A darker color indicates a bigger $S(q)$.

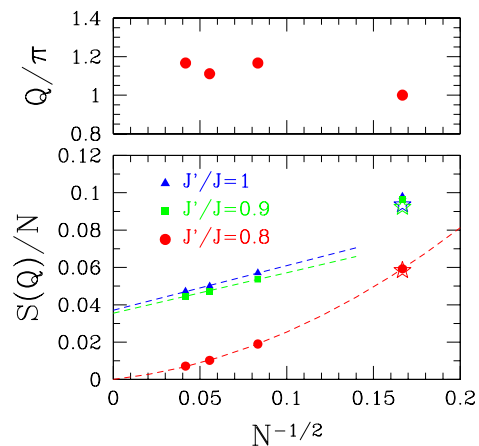


FIG. 5: (Color on-line) Lower panel: size scaling of the magnetic order parameter for different values of J'/J . Stars indicate exact results for $N = 36$ and lines are fits. Upper panel: position of the peak $q = (Q, 0)$ for $J'/J = 0.8$.

inter-chain pairing amplitude. [27]

Let us now move to the magnetic properties that can be assessed by the static spin-spin correlations:

$$S(q) = \frac{1}{N} \sum_{l,m} e^{i\mathbf{q} \cdot (\mathbf{R}_l - \mathbf{R}_m)} \langle \mathbf{S}_l \cdot \mathbf{S}_m \rangle. \quad (3)$$

In Fig. 4, we show the results of $S(q)$ for three typical values of J'/J and three lattice sizes. In the isotropic case, we found that $S(q)$ has huge peaks at the corner of the Brillouin zone. The size scaling of $m^2 = S(Q)/N$ with $Q = (4\pi/3, 0)$ indicates a three-sublattice magnetic order, see Fig. 5. In the thermodynamic limit, we find $m^2 \sim 0.035$, which is larger than $m^2 \sim 0.02$ found in previous works (within the present definition), [9, 10]

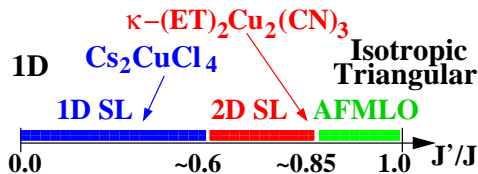


FIG. 6: (Color on-line) Phase diagram of the anisotropic triangular lattice, as obtained by our variational approach.

showing that our approach favors magnetic phases over spin liquids. Despite the fact that the magnetic moment is considerably overestimated, the WF captures correct qualitative features. For $J'/J = 0.9$, we still obtain a finite value of m^2 , which is very close to the one found in the isotropic point. In this case, the peak of $S(q)$ stays at $Q = (4\pi/3, 0)$, very close to the estimation given in Ref. 19. Moreover, another state can be stabilized, with incommensurate Q but slightly higher energy. These facts indicate that the true incommensurability could be very small and it is not detectable with the available sizes. On the other hand, the size scaling at $J'/J = 0.8$ clearly indicates that $m^2 \rightarrow 0$ in the thermodynamic limit. Here, incommensurate spin correlations are found (see Fig. 4), demonstrating the flexibility of the variational WF. Furthermore, for $J'/J \lesssim 0.6$, the spin-spin correlations display an almost 1D character: $S(q)$ does only depend upon q_x , whereas it has a flat behavior as a function of q_y , see Fig. 4. In this regime, the triplet components of the pairing amplitude are irrelevant, and we get a perfect RVB singlet state. Although we cannot exclude a tiny (incommensurate) magnetic order, as it was pointed out in Ref. 20, our calculations highlight the fact that the physical properties in the weakly coupled regime, i.e., $J'/J \lesssim 0.6$, can be effectively represented as a 1D spin liquid down to very low energies (temperatures). On the other hand, for $J'/J \gtrsim 0.6$ triplet components become fundamental to describe magnetic fluctuations. At the same time, for $J'/J \gtrsim 0.6$ also the 2×1 structure of the pairing turns out to be important to gain energy, indicating a (second-order) transition between two spin liquids: one connected to the 1D case, having all equivalent sites, and another one, having a 2×1 structure in the pairing function. No dimer order is found in the whole regime of frustration $0 \leq J'/J \leq 1$.

In summary, by using an improved variational approach, we have given strong evidence that a gapless spin liquid with negligible inter-chain coupling at low energy is stable over a wide region of the anisotropic triangular lattice. The complete phase diagram of this model (see Fig. 6) can be worked out by considering both singlet and triplet pairing amplitudes that may give rise to magnetic order as well as incommensurate spin fluctuations. Our approach highlights the possibility to have two continuous transitions: a first one between two spin liquids and another one from a 2D spin liquid and a magnetic

phase. Close to the isotropic region, triplet correlations are particularly important, without necessarily implying magnetic order. We finally remark that the existence of a non-magnetic state with explicit triplet pairing would naturally lead to a finite susceptibility at zero temperature and the onset of triplet superconductivity, in agreement with NMR experiments in κ -(ET) $_2$ Cu $_2$ (CN) $_3$. [5]

F. Becca thanks R.R.P. Singh for useful discussions at KITP. We acknowledge support from CNR-INFN.

-
- [1] G. Misguich and C. Lhuillier, in “Frustrated Spin Models”, Ed. H. T. Diep, World Scientific, New Jersey (2004).
 - [2] P. Fazekas and P.W. Anderson, *Philos. Mag.* **30**, 423 (1974).
 - [3] P.W. Anderson, *Science* **235**, 1196 (1987).
 - [4] R. Coldea, D.A. Tennant, A.M. Tsvelik, and Z. Tylczynski, *Phys. Rev. Lett.* **86**, 1335 (2001).
 - [5] Y. Shimizu, K. Miyagawa, K. Kanoda, M. Maesato, and G. Saito, *Phys. Rev. Lett.* **91**, 107001 (2003); *Phys. Rev. B* **73**, 140407(R) (2006).
 - [6] P. Mendels, F. Bert, M.A. de Vries, A. Olariu, A. Harrison, F. Duc, J.C. Trombe, J.S. Lord, A. Amato, and C. Baines, *Phys. Rev. Lett.* **98**, 077204 (2007).
 - [7] Y. Okamoto, M. Nohara, H. Aruga-Katori, and H. Takagi, *Phys. Rev. Lett.* **99**, 137207 (2007).
 - [8] B. Bernu, C. Lhuillier, and L. Pierre, *Phys. Rev. Lett.* **69**, 2590 (1992).
 - [9] L. Capriotti, A.E. Trumper, and S. Sorella, *Phys. Rev. Lett.* **82**, 3899 (1999).
 - [10] S.R. White and A.L. Chernyshev, *Phys. Rev. Lett.* **99**, 127004 (2007).
 - [11] O.I. Motrunich, *Phys. Rev. B* **72**, 045105 (2005).
 - [12] P. Sahebsara and D. Senechal, *Phys. Rev. Lett.* **100**, 136402 (2008).
 - [13] K. Foyevtsova, Y. Zhang, H.O. Jeschke, and R. Valenti, arXiv:0812.2197.
 - [14] For a review, see for instance, R.H. McKenzie, *Comments Cond. Matt. Phys.* **18**, 309 (1998).
 - [15] Y. Hayashi and M. Ogata, *J. Phys. Soc. Jpn.* **76** 053705 (2007).
 - [16] S. Yunoki and S. Sorella, *Phys. Rev. Lett.* **92**, 157003 (2004).
 - [17] S. Yunoki and S. Sorella, *Phys. Rev. B* **74**, 014408 (2006).
 - [18] Z. Weihong, R.H. McKenzie, and R.R.P. Singh, *Phys. Rev. B* **59**, 14367 (1999).
 - [19] T. Pardini and R.R.P. Singh, *Phys. Rev. B* **77**, 214433 (2008).
 - [20] M. Bocquet, F.H. Essler, A.M. Tsvelik, and A.O. Gogolin, *Phys. Rev. B* **64**, 094425 (2001).
 - [21] O.A. Starykh and L. Balents, *Phys. Rev. Lett.* **98**, 077205 (2007).
 - [22] M.Q. Weng, D.N. Sheng, Z.Y. Weng, and R.J. Bursill, *Phys. Rev. B* **74**, 012407 (2006).
 - [23] M. Lugas, L. Spanu, F. Becca, and S. Sorella, *Phys. Rev. B* **74**, 165122 (2006).
 - [24] S. Sorella, *Phys. Rev. B* **64**, 024512 (2001).
 - [25] D.A. Huse and V. Elser, *Phys. Rev. Lett.* **60**, 2531 (1988).
 - [26] C. Weber, A. Lauchli, F. Mila, and T. Giamarchi, *Phys. Rev. B* **73**, 014519 (2006).

[27] Residual 2D coupling between chains can be dynamically generated by the Jastrow factor.